Front. Biol. 2013, 8(4): 444–450
DOI 10.1007/s11515-013-1266-y

RESEARCH ARTICLE

Comparative study of the cytotoxicity of the nanosized and microsized tellurium powders on HeLa cells

Huanan WEN[1*], Jiaxin ZHONG[1*], Bei SHEN[1], Tao GAN[1], Chao FU[1], Zhihong ZHU[2], Rui LI (✉)[1], Xu YANG (✉)[1]

[1] *Hubei Key Laboratory of Genetic Regulation and Integrative Biology, College of Life Science, Central China Normal University, Wuhan 430079, China*
[2] *Institute of Nanotechnology, College of Physical Science and Technology, Central China Normal University, Wuhan 430079, China*

Abstract **To compare the cytotoxicity on HeLa cells induced by nanosized and microsized tellurium powders, HeLa cells were exposed to different concentrations of tellurium powders (0, 50, 100, 150 and 200 μg/mL) for 12 h. In this study, detection of a series of biomarkers, including reactive oxygen species (ROS), glutathione (GSH), 8-hydroxy-2'-deoxyguanosine (8-OHdG), in addition to DNA and protein crosslink (DPC) and MTT assay, were conducted to evaluate the cytotoxicity. It is indicated that compared with the control group, there was no significant difference in the induced cytotoxicity at concentrations lower than 50 μg/mL for both nanosized and microsized tellurium powders. While there appears a significant difference in the induced cytotoxicity for nanosized tellurium powders when the concentration is higher than 100 μg/mL as well as for microsized tellurium powders when the concentration is higher than 200 μg/mL. Moreover, it is found that the cytotoxicity induced on HeLa cells exhibits a certain dose-effect relationship with the concentration of tellurium powders. A conclusion has been reached that the toxicity on HeLa cells can be induced by both nanosized and microsized tellurium powders, and the toxicity of the nanosized tellurium powders is significantly greater than the microsized one.**

Keywords nanosized and microsized tellurium powder, HeLa cells, oxidative damage, reactive oxygen species (ROS), glutathione (GSH), DNA and protein crosslink (DPC), 8-hydroxy-2'-deoxyguanosine (8-OHdG)

Introduction

Tellurium (Te) is a rare metalloid element, belonging to VIA group in the periodic table. With a narrow direct band gap of 0.35 eV at room temperature (Liu et al., 2004; Rheem et al., 2010), tellurium is of versatile properties in spite of the size of tellurium, such as photoconductivity, catalytic activity, thermal electricity and strong piezoelectric effect (Ariki and Tanaki 1972; Kudryavstev, 1974; Liu et al., 2004; Liu et al., 2008). In addition, tellurium is also used in agriculture as a component of insecticides (Vij and Hardej, 2012) and in organic tellurium chemistry (Petragnani and Stefani, 2005; Petragnani et al., 2008). With the rapid development of the one-dimensional semiconductor nanostructures, more and more nanosized telluriums are synthesized, including nanowires, nanorods, nanotubes, nanobelts and nanofilms (Liu et al., 2008; Tsiulyanu et al., 2009). Owing to small scale effect, surface effect and quantum effect of nanomaterials, nanosized telluriums exhibit unique physical properties compared with microsized telluriums. For instance, nano-size tellurium-based films and nano-size tellurium-modified silicon nanowires were employed as gas sensors to detect NO_2, NH_3 and $C_3H_7NH_2$, exhibiting lower detection limit and higher sensitivity than microsized tellurium (Yang et al., 201310-11). It is reported that the adverse effect caused by tellurium is characterized by nausea and somnolence (Widy-Tyszkiewicz et al., 2002). The toxicity of tellurium is related to both the chemical form and the consumed quantity of the element. The work conducted by Duckett and Morell demonstrated that tellurium compounds can influence the nervous system (Duckett, 1982; Widy-Tyszkiewicz et al., 2002). A recent study by Valdivia-González et al., (2012) confirmed that tellurite is toxic to the expression and activity of key enzymes of the *E. coli* glycolytic pathway. Never-

Received March 19, 2013; accepted May 3, 2013
Correspondence: [a]Rui LI; [b]Xu YANG
E-mail: [a]ruili@mail.ccnu.edu.cn; [b]yangxu@mail.ccnu.edu.cn
*These authors contributed equally to this work

theless, perhaps similar to cisplatin or carboplatin, coordination compounds of tellurium also have a potential to be anticancer drugs although the mechanism is still evasive (Sredni, 2012). With the increasing application of tellurium, the possibility for people to be exposed to tellurium gets higher; this makes the need for safety evaluation of tellurium impendent. To date, although there are some studies on the safety evaluation of tellurium compounds, little literature is available on the cytotoxicity of nanosized tellurium. To find out a safe limit for the potential application of nanosized tellurium, this study is conducted to explore and compare the toxicity induced by nanosized and microsized tellurium powders on HeLa cells. In the experiment, the reason for choosing HeLa cells is that HeLa cells *in vitro* maintain several features that their originals *in vivo* express under physiological conditions. Furthermore, HeLa cells *in vitro* can be induced by pro-inflammatory compounds to synthesize and release factors that play an important role in the development of diseases. Thus, HeLa cells *in vitro* are a model system suitable for the evaluation of nanoparticles (Kumar, 2006).

According to the work conducted by Roy and Hardej (2011), we set the concentration (0, 50, 100, 150 and 200 μg/mL) of tellurium. In our study, detection of a series of biomarkers, including reactive oxygen species (ROS), glutathione (GSH), 8-hydroxy-2'-deoxyguanosine, in additon to DNA and protein crosslink (DPC) and MTT assay, were conducted to evaluate the toxicity of tellurium on HeLa cells.

Materials and methods

Reagents and apparatus

The nanosized tellurium powder were synthesized by College of Physical Science and Technology of Central China Normal University, the microsized tellurium powders (purity $\geqslant$99.99%) were purchased from Guangzhou Sheng Branch Trade Co., Ltd, 2',7'-dichlorofluorescein (DCF, as diacetate H_2DCF-DA, Calbiochem, brands of EMD Chemicals Inc., an Affiliate of Merck KGaA, Darmstadt, Germany) were used in experiments. All other chemicals used were of analytical grade and were used without further purification. Instruments used in this study include low-temperature refrigerated centrifuge (Eppendorf-5417R), continuous-wave and fluorescent microplate spectrophotometer (Bio-teck FLX800, America), fluorescence spectrophotometer (Hitachi F-4500, Japan) and scanning electron microscope (SEM, JSM-6700F, JEOL).

Characterization of tellurium powder

The morphology of nanosized and microsized tellurium powder were observed and measured under a scaning electron microscope (SEM).

Cell culture and exposure protocol

HeLa cells were cultured in RPMI 1640 medium (GIBCO) supplemented with 10% fetal calf serum (FCS, Sigma), penicillin and streptomycin (each at 100 mU/mL) at 37°C in a humidified atmosphere containing 5% CO_2. The tellurium powder at nano and microscale was dispersed in a complete culture medium with 10% serum to reach final concentrations of 0, 50, 100, 150 and 200 μg/mL according to the work conducted by Shalini Roy (Roy and Hardej, 2011), respectively. Considering the poor solubility of tellurium in media, all media were sonicated for 60 min with the frequency 40 kHz at 20°C prior to the exposure. Cells were then inoculated into the "formulated" medium and incubated at 37°C in a humidified atmosphere containing 5% CO_2 for 12 h. For each concentration of nanosized and microsized tellurium powder, 9 batches of HeLa cell were exposed, respectively. Thus for each index measured in the following experiments, averages and standard deviations were calculated on data obtained from 9 samples and all tests performed in triplicate. For the intracellular ROS detection and MTT assay, the cells were seeded into 96-well plates at a density of 1×10^4 cells/well. In other assays with 24-well plates, the cell density is 1×10^5 cells/well.

Intracellular ROS measurement

The formation of intracellular ROS was measured by monitoring the intensity changes of 2',7'-dichlorofluorescein fluorescence (Li et al., 2010a).

Intracellular GSH measurement

The concentration of intracellular GSH was measured by 5,5'-dithio- bits-(2-nitrobenzoic acid) with modifications on Ping Ma's method (2012) (Ma et al., 2012). The pretreatment of cells is changed as follows: After 12 h incubation in tellurium powder-containing medium, cells in a 24-well plate were washed twice with PBS to remove the tellurium powders and then suspended in 0.5 mL of PBS, following by three circles of freeze at -20°C and thaw at 37°C. After being centrifuged at 3500 r/min for 10 min, the supernatant was collected and detected following Ma's method.

8-Hydroxy-2'-deoxyguanosine detecting assay

The levels of 8-hydroxy-2'-deoxyguanosine (8-OHdG) in the induced cells were detected by enzyme-linked immunosorbent assays (ELISA). A kit (RD Biosciences, San Diego, CA 92121, USA) specific for mice 8-OHdG was used. All procedures were conducted according to the manufacturer's instructions. Yellow-colored product formed in proportion to the amount of 8-OHdG present in the samples and standards. The standard curve equation for the 8-OHdG test is as follows: C (pg/mL) = 163.94 × OD – 70.87.

DNA and protein crosslink (DPC) assay

KCl-SDS method (Li et al., 2010b) was used to detect DNA damage. DPC coefficient was calculated as a ratio the percentage of the DNA involved in DPC over the percentage of the DNA involved in DPC plus the unbound DNA fraction.

MTT assay

The MTT assay was applied to investigate the cytotoxicity of tellurium powders following Li's method (Li et al., 2010a), with the exposure time elongated to 12 h.

Data analysis

All data were analyzed and plotted using Origin 6.0software. Before performing any analyses, all data were assessed for normal distribution. Thereafter, both a oneway analysis of variance (ANOVA) and a Tukey test were applied to evaluate significant differences. A p value less than 0.05 or 0.01 were used to evaluate statistical significance.

Results

Characterization of the nanosized and microsized tellurium powders

The oxidative damage induced by tellurium powders is highly related to their size and structure (Rejman et al., 2004; Kumar, 2006), which was examined by SEM. Figure 1A showed that the nanosized tellurium were clavate in shape with diameter of 90–270 nm and length of 1–1.5 μm. Figure 1B showed that the microsized tellurium were near-spherical in shape with diameter of 6–9 μm.

Intracellular ROS generation

The result of intracellular ROS concentration induced by different doses of nanosized and microsized tellurium powders is shown in Fig. 2. It is obvious that with the increase in the concentration of tellurium powders, there is an increasing tendency of the ROS content. Compared with the control group, when the concentratoin is higher than100 μg/mL for the nanosized tellurium, the ROS levels were significantly increased ($p < 0.01$); as for microsized tellurium, the excess ROS was not induced compared with the control until the concentration is over 150 μg/mL (200 μg/mL, $p < 0.05$). In addition, there is significantly difference in the ROS level induced by nanosized and microsized tellurium powders, even at the same concentration.

GSH content

Figure 3 presents the relationship between GSH content and different concentrations of tellurium powders. With the increasing concentration of tellurium powders, there is a decreasing tendency of the GSH content. Compared with the control group, at $\geqslant$100 μg/mL of nanosized tellurium, the GSH contents were significantly decreased (100, 150 and 200 μg/mL, $p < 0.01$); however, at 200 μg/mL, the GSH content increases little compared with 150 μg/mL. As for microsized tellurium, the GSH content was not induced compared with the control until the concentration is 200 μg/mL (200 μg/mL, $p < 0.05$). In addition, there is a significant difference in the GSH content induced by nanosized and microsized tellurium powders, at the same concentration higher than 100 μg/mL ($p < 0.01$).

8-OHdG content

The change of 8-hydroxy-2'-deoxyguanosine contents is shown in Fig. 4. Induced by nanosized tellurium powders,

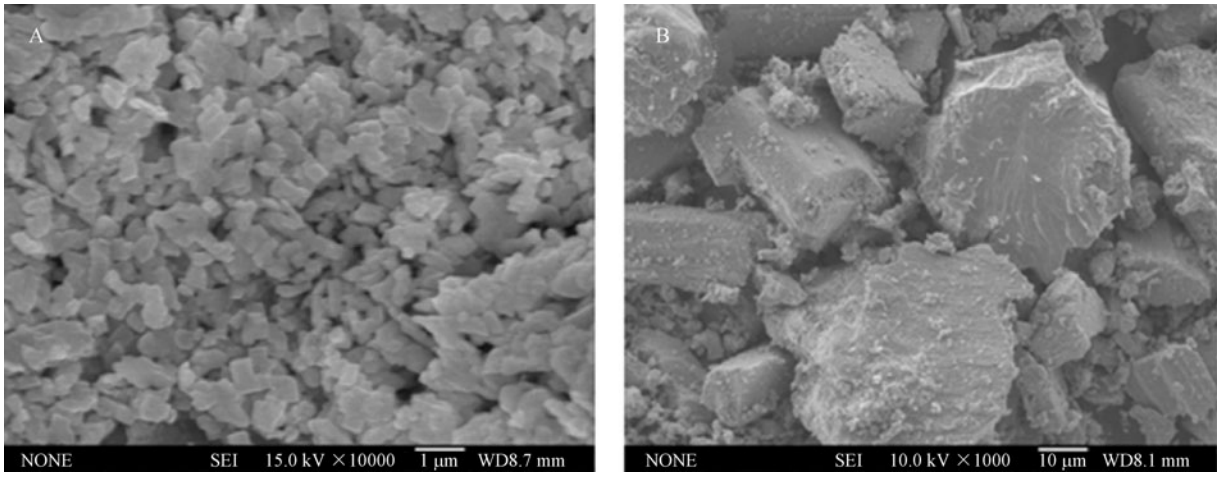

Figure 1 Morphology of the tested materials (SEM). (A) Nanosized tellurium powders; (B) Microsized tellurium powders

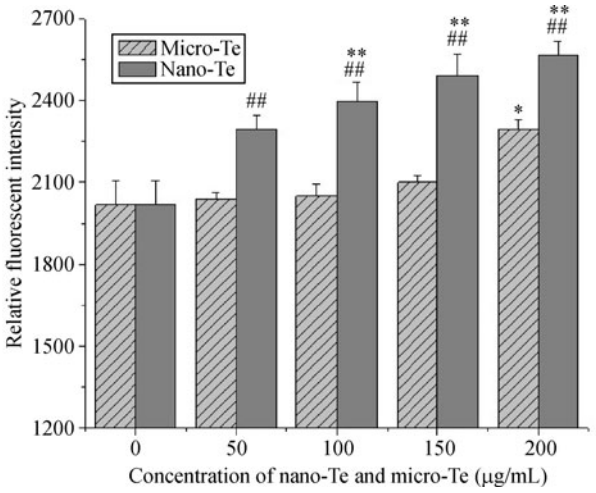

Figure 2 DCF-fluorescence intensity induced by different concentrations of nanosized and microsized tellurium powders. Results are the mean±SD (n = 9). (*: $p < 0.05$ and **: $p < 0.01$, compared with the control group; #: $p < 0.05$ and ##: $p < 0.01$, compared with microsized tellurium treated groups)

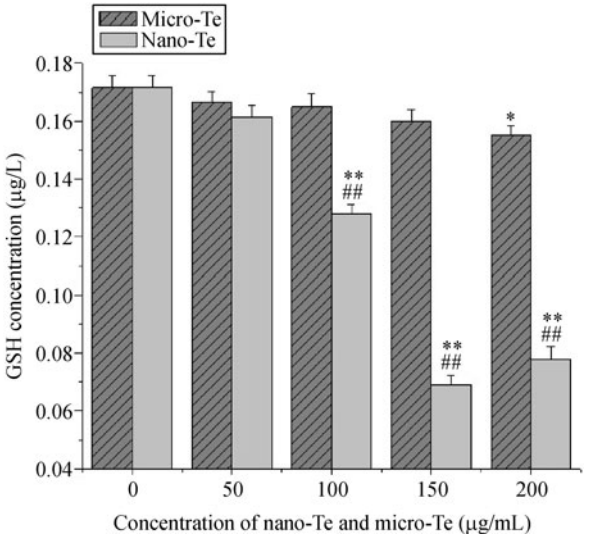

Figure 3 GSH contents induced by different concentrations of nanosized and microsized tellurium powders. Results are the mean ±SD (n = 9). (*: $p < 0.05$ and **: $p < 0.01$, compared with the control group; #: $p < 0.05$ and ##: $p < 0.01$, compared with microsized tellurium treated groups)

the 8-OHdG contents were significantly increased compared with the control group (100 μg/mL, $p < 0.05$; 150 and 200 μg/mL, $p < 0.01$). As for microsized tellurium powders, the 8-OHdG contents change was not significant compared with the control until the concentration is over 150 μg/mL (200 μg/mL, $p < 0.05$). In addition, there is significantly difference in the 8-OHdG content induced by nanosized and microsized tellurium powders, at the same concentration (50 μg/mL, $p < 0.05$; 100, 150 and 200 μg/mL, $p < 0.01$).

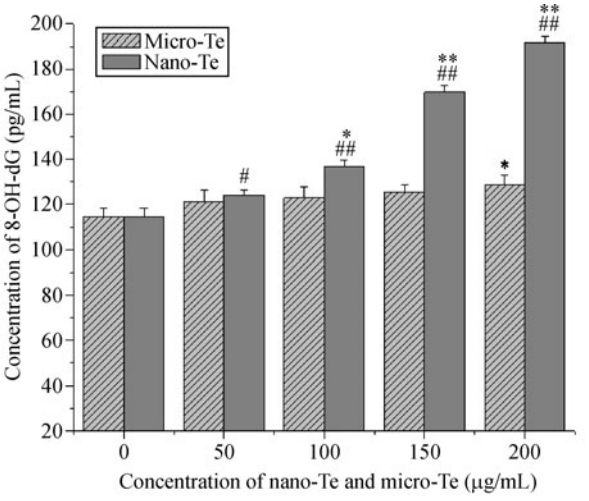

Figure 4 8-OHdG contents induced by different concentrations of nanosized and microsized tellurium powders. Results are the mean±SD (n = 9). (*: $p < 0.05$ and **: $p < 0.01$, compared with the control group; #: $p < 0.05$ and ##: $p < 0.01$, compared with microsized tellurium treated groups)

DNA–protein cross-linking coefficient

Figure 5 demonstrated that DPC coefficients were increased with the growing concentrations of tellurium powders. In addition, there is significantly difference in the DPC coefficient induced by nanosized and microsized tellurium powders, at the same concentration (50 μg/mL and 100 μg/mL, $p < 0.05$; 150 and 200 μg/mL, $p < 0.01$).

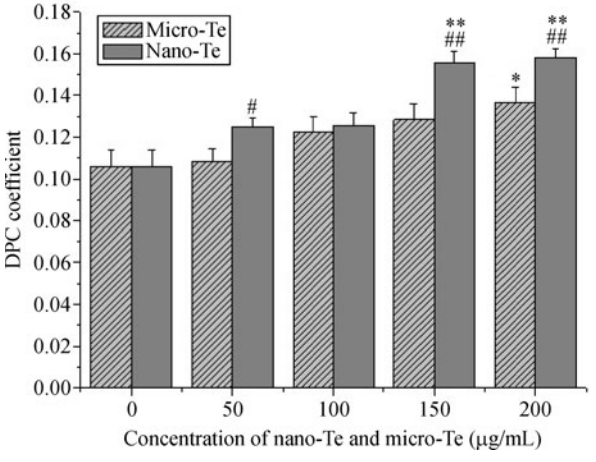

Figure 5 DPC coefficients induced by different concentrations of nanosized and microsized tellurium powders. Results are the mean±SD (n = 9). (*: $p < 0.05$ and **: $p < 0.01$, compared with the control group; #: $p < 0.05$ and ##: $p < 0.01$, compared with microsized tellurium treated groups)

MTT assay

The MTT assay indicated the cell viability induced by different concentrations of nanosized and microsized tell-

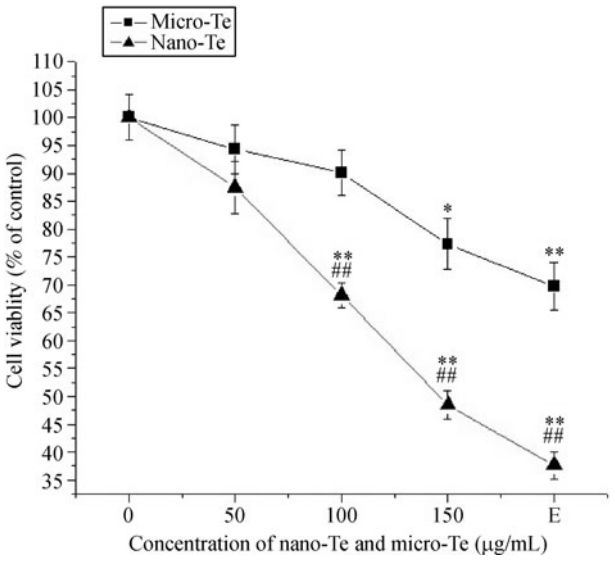

Figure 6 Effects of tellurium on the cell viability of HeLa cells. Cell viability was determined by the MTT assay. Results are the mean±SD (n = 9). (*: $p < 0.05$ and **: $p < 0.01$, compared with the control group; #: $p < 0.05$ and ##: $p < 0.01$, compared with microsized tellurium treated groups)

urium powders. With the increase in the concentration of tellurium powders, the cell viability decreased significantly. There is also significantly difference in the cell viability induced by nanosized and microsized tellurium powders, at the same concentration higher than 100 μg/mL ($p < 0.01$).

Discussion

In this study, the detection of ROS, GSH, 8-OHdG, DPC and MTT assay were used to explore and compare the toxicity on HeLa cells induced by different concentrations of nanosized and microsized tellurium powders. The results of ROS and GSH change suggest that HeLa cells can be resistant to low concentrations of tellurium powders. However, once the concentration is higher, there will be excess reactive oxygen species generation and a significant depletion of GSH contents. However, HeLa cells exhibited higher tolerance to microsized tellurium powders than nanosized counterparts. As Nel and Kovochich pointed out (Nel et al., 2006; Xia et al., 2006), ROS and oxidative stress compose the main elements of cytotoxicity caused by nanomaterials. Taking the chemical properties of element tellurite and the structure of nanosized tellurium into account, as a p-type semiconductor with a narrow band gap (Liu et al., 2004; She et al., 2009), tellurium is easy to be excited by light to produce highly active electrons which can react with hydroxy to generate hydroxide radical. Futhermore, the specific structure characteristics of nanomaterials, such as the discontinuous crystal planes and surface defects, can generate active electron configuration which could facilitate the transformation of oxygen into hydroxide radical. This probably provides a reason why there is excesive ROS induced by nanosized tellurium powders than microsized one. It is necessary to maintain the normal ROS level in cells since it is coupled with a series of signal transduction pathways (Das et al., 1999, 2005; Chen et al., 2003). Once the ROS is excess, damages to large biomoleucles including DNA, protein and lipids will be caused (Wang et al., 2011; Gałazyn-Sidorczuk et al., 2009). The balance of oxidants and antioxidants is of much importance in cells. As a small molecular scavenger, GSH can eliminate free radicals. Therefore, the content of GSH can be as an indicator of the antioxidant capacity. Our data confirmed that the GSH depletion is in line with the excess ROS and the oxidative damages induced by nanosized tellurium powders is greater than microsized one. Moreover, the GSH content induced by nanosized tellurium powders in 200 μg/mL group is higher than 150 μg/mL. We tentatively put forward that with the concentration increase, the nanosized tellurium powders are easy to agglomerate so that its size will be beyond the micorsize.To further verify the oxidative damages, the detection of 8-OHdG content and DNA–protein cross-linking coefficient is essential. As one of the targets of ROS, 8-OHdG can cause nucleotide mismatch and gene mutation. When the ROS is redundant, the balance of oxidants and antioxidants will be disrupted. With the GSH exhausted, the excess ROS will attack DNA to generate 8-OHdG and DNA–protein cross-linking. 8-OHdG can be cleared by base excision repair and its contents can reflect the degree of oxidative damages. Hence, 8-OHdG can be a biomarker of oxidative stress to DNA (Wu et al., 2004; Au et al., 2009). In addition, free radical can also lead proteins to crosslink to DNA through oxidative stress (Zhang and Wheeler, 1993). The result of 8-OHdG contents change is consistant with the change of ROS level. The rising trend of DPC coefficient as the concentration of the administered tellurium powder increase, also help to confirm that DNA damage from DPC was heavily depressed (Kagan et al., 2006). Moreover, the cell viability is highly related to the oxidative damages induced by tellurium powders. In the MTT assay, the viability of HeLa cells exposed to microsized powder is much higher than that of the nanosized one. The results may be attributed to the strong oxidative stress caused by nanomaterials. The nanomaterials with high reactivity can interact with cell membrane to generate ROS, and then the oxidative stress aroused by ROS can lead to the membranolysis and break of calcium homeostasis, which further activate the endonuclease depending on the calcium concentration, and finally result in the cell apoptosis (Rahman et al., 2002). In summary, the toxicity on HeLa cells can be induced by both nanosized and microsized tellurium powders, and the toxicity caused by the nanosized Tellurium powders is significantly greater than that caused by the microsized one. It should be noted that this study focuses on only the cell experiment, and the *in vivo* study with mice will be the topic of our next study.

Acknowledgements

This work was supported by the grants of the National Natural Science Foundation of China (Grant No. 21103059) and the Innovative Experiment Program for University Students of Chinese Ministry of Education.

Compliance with ethics guidelines

Huanan Wen, Jiaxin Zhong, Bei Shen, Tao Gan, Chao Fu, Zhihong Zhu, Rui Li, Xu Yang declare that they have no conflict of interest. This article does not contain any studies with human or animal subjects performed by any the authors.

References

Ariki K, Tanaki T (1972). Piezoelectric and elastic properties of single crystalline Se-Te alloys. Jpn J Appl Phys, 11(4): 472–479

Au W W, Oberheitmann V, Harm C (2009). Assessing DNA damage and health risk using biomarkers. Mutat Res, 509(1): 153–163

Chen K, Thomas S R, Keaney J F Jr (2003). Beyond LDL oxidation: ROS in vascular signal transduction. Free Radic Biol Med, 35(2): 117–132

Das D K, Maulik N, Sato M, Ray P S (1999). Reactive oxygen species function as second messenger during ischemic preconditioning of heart. Mol Cell Biochem, 196(1-2): 59–67

Das M, Babu K, Reddy N P, Srivastava L M (2005). Oxidative damage of plasma proteins and lipids in epidemic dropsy patients: alterations in antioxidant status. Biochim Biophys Acta, 1722(2): 209–217

Duckett S (1982). The distribution and localization of 127m tellurium in normal and pathological nervous tissues of young and adult rats. Neurotoxicology, 3(3): 63–73

Gałazyn-Sidorczuk M, Brzóska M M, Jurczuk M, Moniuszko-Jakoniuk J (2009). Oxidative damage to proteins and DNA in rats exposed to cadmium and/or ethanol. Chem Biol Interact, 180(1): 31–38

Kagan V E, Tyurina Y Y, Tyurin V A, Konduru N V, Potapovich A I, Osipov A N, Kisin E R, Schwegler-Berry D, Mercer R, Castranova V, Shvedova A A (2006). Direct and indirect effects of single walled carbon nanotubes on RAW 264.7 macrophages: role of iron. Toxicol Lett, 165(1): 88–100

Kudryavstev A A (1974). The Chemistry and Technology of Selenium and Tellurium. London: Collet's Ltd.

Kumar C S S R (2006). Nanomaterials-Toxicity, Health and Environment Issues. Nanotechnologies for the Life Science, 5

Li Y, Liu D, Ai H H, Chang Q, Liu D, Xia Y, Liu S, Peng N, Xi Z, Yang X (2010b). Biological evaluation of layered double hydroxides as efficient drug vehicles. Nanotechnology, 21(10): 105101

Li Y, Tian X K, Lu Z S, Yang C, Yang G, Zhou X, Yao H, Zhu Z, Xi Z, Yang X (2010a). Mechanism for α-MnO2 nanowire-induced cytotoxicity in Hela cells. J Nanosci Nanotechnol, 10(1): 397–404

Liu H M, Liu S X, Huang K X (2008). Low-temperature chemical route to bismuth-doped tellurium sing-crystalline nanorods. Mater Lett, 62 (12): 1983–1985

Liu X Y, Mo M S, Chen X Y, Qian Y (2004). A ratioal redox route for the synthesis of tellurium nanotubes. Inorg Chem Commun, 7(2): 257–259

Ma P, Luo Q, Chen J Y, Gan Y, Du J, Ding S, Xi Z, Yang X (2012). Intraperitoneal injection of magnetic Fe_3O_4-nanoparticle induces hepatic and renal tissue injury via oxidative stress in mice. Int J Nanomedicine, 7: 4809–4818

Nel A, Xia T, Mädler L, Li N (2006). Toxic potential of materials at the nanolevel. Science, 311(5761): 622–627

Petragnani N, Mendes S R, Silvira C C (2008). Tellurium tetrachloride: an improved method of preperation. Tetrahedron Lett, 49(15): 2371–2372

Petragnani N, Stefani H A (2005). Advances in organic tellurium chemistry. Tetradron, 61(7): 1613–1679

Rahman Q, Lohani M, Dopp E, Pemsel H, Jonas L, Weiss D G, Schiffmann D (2002). Evidence that ultrafine titanium dioxide induces micronuclei and apoptosis in Syrian hamster embryo fibroblasts. Environ Health Perspect, 110(8): 797–800

Rejman J, Oberle V, Zuhorn I S, Hoekstra D (2004). Size-dependent internalization of particles via the pathways of clathrin- and caveolae-mediated endocytosis. Biochem J, 377(Pt 1): 159–169

Rheem Y, Chang C H, Hangarter C M, Park D Y, Lee K H, Jeong Y S, Myung N V (2010). Synthesis of tellurium nanotubes by galvanic displacement. Electrochim Acta, 55(7): 2472–2476

Roy S, Hardej D (2011). Tellurium tetrachloride and diphenyl ditelluride cause cytotoxicity in rat hippocampal astrocytes. Food Chem Toxicol, 49(10): 2564–2574

She G W, Shi W S, Zhang X, Wong T, Cai Y, Wang N (2009). Template-free electrodepasition of one-dimensional nanostructures of tellurium. Cryst Growth Des, 9(2): 663–666

Sredni B (2012). Immunomodulating tellurium compounds as anti-cancer agents. Semin Cancer Biol, 22(1): 60–69

Tsiulyanu D, Marian T, Tiuleanu A, Liess H D, Eisele I (2009). Effect of aging and temperature on alternating current conductivity of Tellurium thin films. Thin Solid Films, 517(8): 2820–2823

Tsiuyanu D, Tsiulyanu A, Liess H D, Eisele I (2005). Characterization of tellurium-based films for NO_2 detection. Thin Solid Films, 485(1): 252–256

Valdivia-González M, Pérez-Donoso J M, Vásquez C C (2012). Effect of tellurite-mediated oxidative stress on the *Escherichia coli* glycolytic pathway. Biometals, 25(2): 451–458

Vij P, Hardej D (2012). Evaluation of tellurium toxicity in transformed and non-transformed human colon cells. Environ Toxicol Pharmacol, 34(3): 768–782

Wang X, Liu J Z, Hu J X, Wu H, Li Y L, Chen H L, Bai H, Hai C X (2011). ROS-activated p38 MAPK/ERK-Akt cascade plays a central role in palmitic acid-stimulated hepatocyte proliferation. Free Radic Biol Med, 51(2): 539–551

Widy-Tyszkiewicz E, Piechal A, Gajkowska B, Smiałek M (2002). Tellurium-induced cognitive deficits in rats are related to neuropathological changes in the central nervous system. Toxicol Lett, 131 (3): 203–214

Wu L L, Chiou C C, Chang P Y, Wu J T (2004). Urinary 8-OHdG: a marker of oxidative stress to DNA and a risk factor for cancer, atherosclerosis and diabetics. Clin Chim Acta, 339(1-2): 1–9

Xia T, Kovochich M, Brant J, Hotze M, Sempf J, Oberley T, Sioutas C,

Yeh J I, Wiesner M R, Nel A E (2006). Comparison of the abilities of ambient and manufactured nanoparticles to induce cellular toxicity according to an oxidative stress paradigm. Nano Lett, 6(8): 1794–1807

Yang L, Lin H Y, Zhang Z S, Cheng L, Ye S, Shao M (2013). Gas sensing of tellurium-modified silicon nanowires to ammonia and propylamine. Sens Actuators B Chem, 177(2): 260–264

Zhang H, Wheeler K T (1993). Radiation-induced DNA damage in tumors and normal tissues. I. Feasibility of estimating the hypoxic fraction. Radiat Res, 136(1): 77–88